A Guideline for Low-Force Robotic Guidance for Enhancing Human Performance of Positioning and Trajectory Tracking: It Should Be Stiff and Appropriately Slow

Ryo Kikuuwe, *Member, IEEE*, Takahiro Yamamoto, and Hideo Fujimoto

***Abstract*—This paper considers the application of a low-force robotic manipulator to guide a human user's movements to place a tool (or the user's hand) at a predetermined position or move it along a predetermined trajectory. This application is potentially useful, e.g., skill training for humans, rehabilitation, and human–machine coordination in the manufacturing industry. A proportional-derivative (PD)-type position control can be used for this application, but the parameters for the controller should be appropriately chosen for enhancing the human performance of positioning and trajectory tracking. We hypothesize that the robot's position control should be stiff and appropriately slow, i.e., the proportional gain should be high and the time constant (the ratio of the derivative gain to the proportional gain) should be appropriately large. Such characteristic has been difficult to be realized in ordinary PD position control because it requires direct high-gain velocity feedback. However, our recent technique, which is proxy-based sliding mode control (PSMC), is capable of producing such a hypothetically preferred response and allows us to empirically validate the hypothesis. The results of experiments using two distinctly different robotic devices supported the hypothesis, showing that the time constant should be set around 0.1 s rather than 0.01 and 0.5 s.**

***Index Terms*—Guidance, human–machine coordination, proxy-based sliding mode control (PSMC), time constant.**

NOMENCLATURE

The following symbols appear throughout this paper:

$\boldsymbol{f}$	The force from the robot to the controlled object.
$\boldsymbol{h}$	The force from the human user to the controlled object.
$\boldsymbol{p}$	The actual position of the controlled object.
$\boldsymbol{p}_d$	The desired position of the controlled object.
$\boldsymbol{p}_s$	The position of the proxy, which is used in proxy-based sliding mode control (PSMC).
F	The upper limit of the magnitude of $\boldsymbol{f}$.
F_τ	The upper limit of the joint torque of the robot.
K	The proportional gain for PSMC and PD control.
H	The time constant for PSMC and PD control.
T	The sampling interval for PSMC.
B	The derivative gain for PSMC.

Manuscript received December 27, 2006; revised June 19, 2007. This paper was presented in part at the 14th Symposium on Haptic Interfaces for Virtual Environments and Teleoperator Systems, Alexandria, VA, March 2006. This paper was recommended by Associate Editor R. Hess.

R. Kikuuwe is with Kyushu University, Fukuoka 819-0395, Japan (e-mail: kikuuwe@ieee.org).

T. Yamamoto is with the Nagoya Institute of Technology, Nagoya 466-8555, Japan.

H. Fujimoto is with the Graduate School of Engineering and Quality Innovation Techno-Center, Nagoya Institute of Technology, Nagoya 466-8555, Japan.

Digital Object Identifier 10.1109/TSMCA.2008.923085

I. INTRODUCTION

HUMANS and robots have different capabilities. One of the major ideas of human–robot coordination is to use a robot as a powerful assistant loyal to the intention of a human user [2]–[6]. In such applications, a human makes decisions, whereas a robot produces power. Opposite to this is the approach in which the human produces power, whereas a robot (or a device) produces some small forces only for enhancing accuracy and/or safety. For example, robotic devices can be used to produce some appropriate resistive forces, such as Coulomb-like friction force, for stabilizing manual tasks [7]. In the field of aviation, stick controllers that actively produce resistive forces have been developed for the purpose of improving tracking performance [8], [9]. Some recent researchers are investigating the use of haptic devices for displaying virtual walls to constrain the user on a predetermined path or to prevent the user from touching predetermined regions [10]–[13].

This paper considers a class of human–machine coordination that can fall into the latter category but is slightly different from those described earlier. Specifically, we consider the following situation.

1) A human user is requested to place his/her hand (or a grasped tool) at a given position or to move his/her hand along a given trajectory.
2) A robot actively produces small forces to guide the human user's hand toward the desired position or along the desired trajectory, as shown in Fig. 1.
3) The user knows and can visually recognize the desired position or trajectory.
4) The data of the desired position or trajectory are provided to the robot controller in advance.
5) The robot's actuator force is so small that the user can easily deviate from the desired trajectory when she/he intends to do so.

We refer to this application of a robot as low-force kinesthetic guidance. The application of robotic devices for guiding human movements has been investigated by several researchers for the purposes of skill training [14]–[17], haptic cueing [18],

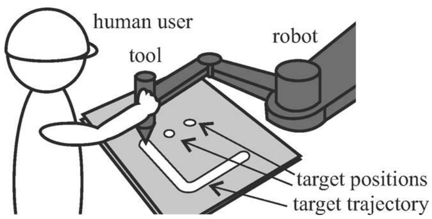

Fig. 1. Kinesthetic guidance.

and rehabilitation of upper limb function [19]–[22]. In such cases, a low-powered/low-force robot will be preferred for safety reasons and for allowing the user to move against the guidance when necessary. Active guidance will be preferred to passive guidance (such as virtual walls) if the desired position or trajectory changes according to time.

The low-force kinesthetic guidance scheme has some potential applications also in the manufacturing industry. This scheme can be applied to the processes of, for example, cutting, welding, painting, drawing, and adhesive application at specified spots or along a specified trajectory. Because the desired position or trajectory is predetermined, full automation without human involvement may be technically possible. However, the low-force kinesthetic guidance scheme can be a solution to remove the spatial isolation of high-powered robots from human workspace. The isolation of human workers from high-powered robots is usually obliged for the workers' safety. It requires a large site area and is inconvenient if the task to be executed by the robot has some subordinate tasks that require human involvement, such as visual/haptic inspection, tool changing, and fine adjustment.

The central question addressed in this paper is what kind of control scheme is suitable for low-force kinesthetic guidance. Because the desired position is provided to the robot controller in advance, it is technically easy to apply ordinary proportional-derivative (PD) control. For enhancing human performance, however, the parameters for the controller should be carefully chosen particularly under the limitation of the robot's actuator force. As a potential solution for this problem, we hypothesize that the guidance should be stiff and appropriately slow. Specifically, the stiffness should be as high as permitted by the control stability [12], [23], and the slowness should be around 0.1 s in terms of time constant. High stiffness will be necessary for suppressing the influence of disturbance. Being appropriately slow will be necessary because abrupt changes in guiding force will not be able to influence the user's motion, causing the separation of the user's position from the desired position. On the other hand, being too slow will not be preferred because it will impede the user's faster motions. The main contribution of this paper is the empirical validation of this hypothesis.

Aside from the validity of the hypothesis, realizing slow response characteristic combined with high stiffness in position control is technically difficult because it requires a high-gain velocity feedback, which cannot practically be used because the velocity signal is usually noisy. This difficulty, however, can now be removed by using a PSMC scheme [24], which was recently proposed by the authors. Without using high-gain velocity feedback, PSMC responds slowly, in an overdamped manner, to large positional errors caused by actuator force saturation. It however responds fast to small positional errors, as long as the actuator force is below the saturation level, and thus, it is as accurate as ordinary high-gain PD control. Our initial purpose of developing PSMC was enhancing safety of general position-controlled robots without sacrificing control performance. This paper on kinesthetic guidance was motivated by an incidental finding that the slow response produced by PSMC was subjectively felt easy to follow when the authors held the robot's end effector and moved together. This paper presents the experimental results on low-force kinesthetic guidance of positioning and trajectory-tracking tasks by using PSMC as a tool for producing slow response. The results support the validity of the hypothesis.

The rest of this paper is organized as follows. Section II defines the problem to be addressed and presents a hypothesis as a possible solution to the problem. In addition, this section overviews the previously proposed PSMC scheme as a technical tool for testing the hypothesis. Sections III and IV present the experimental results of positioning and trajectory-tracking tasks, respectively, using a large parallel link manipulator. Section V presents another two sets of experiments using a lightweight robotic device. Section VI provides the concluding remarks.

II. Low-Force Kinesthetic Guidance

A. Problem

Let us consider the situation where a robot and a human user are applying forces to an object to move it toward a desired position in the n-dimensional Cartesian space. Moreover, let us assume that the control law of the robot is a simple PD-type position control law with force saturation. The problem addressed in this paper is what values are suitable for the gains of the PD-type position controller in this situation.

In the situation described earlier, the equation of motion of the carried object is described as follows:

$$M\ddot{\boldsymbol{p}} = \boldsymbol{f} + \boldsymbol{h} + \boldsymbol{d}. \tag{1}$$

Here, $M > 0$ denotes the mass of the object, and $\boldsymbol{p} \in \mathbb{R}^n$ denotes the position of the object. The vectors $\boldsymbol{f} \in \mathbb{R}^n$ and $\boldsymbol{h} \in \mathbb{R}^n$ represent the forces applied to the object from the robot and the human user, respectively. The vector $\boldsymbol{d} \in \mathbb{R}^n$ represents the disturbance, which is the sum of forces resulted from all external sources and unmodeled factors such as nonlinearities.

The PD-type position controller with force saturation, which is implemented in the robot, is described as follows:

$$\boldsymbol{f} = F\mathbf{sat}\left(K\left(\boldsymbol{p}_d - \boldsymbol{p} + H(\dot{\boldsymbol{p}}_d - \dot{\boldsymbol{p}})\right)/F\right). \tag{2}$$

Here, $\boldsymbol{p}_d \in \mathbb{R}^n$ denotes the desired position of the object, and F, K, and H are positive real numbers. The function $\mathbf{sat} : \mathbb{R}^n \to \mathbb{R}^n$ is the unit saturation function defined as follows:

$$\mathbf{sat}(\boldsymbol{x}) = \begin{cases} \boldsymbol{x}, & \text{if } \|\boldsymbol{x}\| \leq 1 \\ \boldsymbol{x}/\|\boldsymbol{x}\|, & \text{if } \|\boldsymbol{x}\| > 1. \end{cases} \tag{3}$$

The motivation for (2) can be understood by noticing that the function $\mathbf{sat}$ satisfies the following:

$$X\mathbf{sat}(\boldsymbol{x}/X) = \begin{cases} \boldsymbol{x}, & \text{if } \|\boldsymbol{x}\| \leq X \\ X\boldsymbol{x}/\|\boldsymbol{x}\|, & \text{if } \|\boldsymbol{x}\| > X \end{cases} \tag{4}$$

for all $X > 0$ and $\boldsymbol{x} \in \mathbb{R}^n$. It is thus clear that the control law (2) is the force-limited PD control law of which the proportional gain is K, the derivative gain is KH, and the force limit is F. The parameter H is usually referred to as the (derivative) time constant, which determines how slow the controller responds.

It is straightforward to imagine that the force limit F can be chosen by considering the safety of the users or the limitations of the hardware. The problem addressed in this paper is specifically what values are suitable for the proportional gain K and the time constant H.

B. Hypothesis and Its Rationale

As a potential solution for the problem described in Section II-A, we hypothesize that, in the control law (2), K should be as high as possible and H should be an appropriate value, which is specifically around 0.1 s. We provide here a possible rationale for this hypothesis.

The necessity for high stiffness K can be intuitively understood because it generally contributes to the reduction of the influence of disturbances. The necessity for an appropriate value for H can be justified because both too large and too small values of H will produce undesirable effects. Notice that the control law (2) produces zero actuator force ($\boldsymbol{f} = \boldsymbol{o}$, where $\boldsymbol{o}$ denotes the n-dimensional zero vector) if $\boldsymbol{p}$ is moving in the following trajectory:

$$\boldsymbol{p} = \boldsymbol{p}_d + ((\boldsymbol{p} - \boldsymbol{p}_d)|_{t=t_0}) \exp\left(-(t - t_0)/H\right) \tag{5}$$

where t_0 is an arbitrary time. This equilibrium position profile represents an exponential converging motion toward the desired position $\boldsymbol{p}_d$, and the time constant H characterizes how slow this convergence is. Imagine that the human user's movement toward $\boldsymbol{p}_d$ is faster than the equilibrium trajectory (5). In this situation, the robot will resist the user's movement and can cause extra fatigue to the user. On contrary, imagine that the user's movement is slower than the equilibrium trajectory (5). In this situation, the robot will pull the user toward $\boldsymbol{p}_d$ even when she/he is decelerating to stop at $\boldsymbol{p}_d$, causing overshoots. Thus, we can speculate that some middle value will be suited for H for the use of low-force kinesthetic guidance. If the user is moving almost in the same trajectory as (5) and the stiffness K is sufficiently high, the robot's force is produced only for preventing the user from moving away from the trajectory (5) by canceling disturbances from his/her neuromuscular system and external physical sources.

We now consider under what value of H the trajectory (5) becomes similar to that of human voluntary movements. In a reaching movement toward a given target position, a human generally produces a smooth bell-shaped velocity profile [25], [26]. The position profile of a reaching movement, which is the first-order integral of a bell-shaped profile, is somewhat different from the trajectory in (5), but at least, the latter part of the profile exhibits smooth convergence, which is similar to that of the exponential function (5). By approximating the user's reaching movement in (5), we can view the user as a first-order lag element with a time constant of H, which accepts the desired position $\boldsymbol{p}_d$ as the input and provides the actual position $\boldsymbol{p}$ as the output.

The literature includes several reports regarding the time constant of human response. Happee [27] investigated human movements toward a target position and modeled a human as an optimal controller that produces a force output. In his model, the controller output is originally discontinuous, but it was smoothed by a first-order lag element representing some neuromuscular dynamics. The time constant of the lag element is empirically identified as 0.05 to 0.14 s. Kleinman *et al.* [28] investigated the human control strategy of operating a vehicle (an aircraft) and modeled a human operator as an element that provides the displacement of the control stick of an aircraft as an output. In their model, the human operator is an optimal linear state feedback controller of which the output is filtered through a first-order lag element. Their survey of studies mainly at the U.S. Air Force in 1950s and 1960s (e.g., [29]) suggests that the time constant is on the order of 0.07 to 0.3 s.

We can further speculate that the time constant may be related to the bandwidth of human voluntary movements. Mann *et al.* [30] have shown that the predominant frequency component of the wrist motion for 24 activities of daily living is 1 Hz, and 75% of the spectral energy is less than 5 Hz. Hollerbach [31] has reported that the hand movements during writing letters are around 6 Hz. Riviere *et al.* [32] have reported that, in simulated microsurgery performed by trained eye surgeons, 98.9% of the total power of voluntary movements was below 2 Hz. When a human is viewed as a first-order lag element from the desired (intended) position to the actual position, the aforementioned literature survey indicates that its cutoff frequency is roughly around 2 Hz, which corresponds to the time constant of $1/(2\pi \times 2) \approx 0.1$ s.

As discussed earlier, the literature suggests that we can use 0.1 s as a typical value of the time constant of human response and can hypothesize that $H = 0.1$ s is an appropriate choice for low-kinesthetic guidance. The choice of $H = 0.1$ s is not precise; at this time, we can only say that $H = 0.1$ s could be better than, for example, 0.01 and 0.5 s, which are not included in the ranges of time constants described in the literature. Nevertheless, the aforementioned rationale for the hypothesis definitely remains to be validated through more complete analyses from the control-theoretic and physiological aspects. Such analyses will not be straightforward because the control strategy behind the neuromuscular lag element is not clear and the actuator force saturation in (2) makes the entire system nonlinear [33], [34]. Leaving such analyses outside the scope of this paper, this paper concentrates on the empirical validation of the hypothesis.

C. Technical Challenge and Its Solution: PSMC

The hypothesis in Section II-B suggests that the PD-type position controller for kinesthetic guidance requires its proportional gain K to be high and its time constant H to be

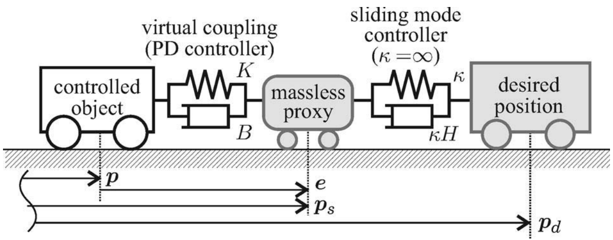

Fig. 2. Physical interpretation of PSMC [24].

around 0.1 s. Aside from the validity of this hypothesis, it is technically difficult to combine high stiffness with 0.1-s time constant because this combination requires the gain KH of the derivative (velocity) feedback to be high. The velocity signal is usually noisy due to discrete measurement of position and time. Although there are some filtering techniques to attenuate the discretization errors [35], high-gain velocity feedback is still practically difficult. Moreover, high-gain velocity feedback will deteriorate the tracking performance even below the force limit.

The technical difficulty in combining high stiffness and slow response in position control has been overcome by the proxy-based sliding mode control (PSMC) scheme, which has been proposed in a previous paper [24] of the authors. Fig. 2 shows the underlying concept of PSMC. The controlled object is connected to a massless virtual object, which is referred to as proxy, through a virtual spring-damper element, which is referred to as virtual coupling.[1] Thus, the force $\boldsymbol{f}$ that acts from the proxy to the virtual coupling is written as follows:

$$\boldsymbol{f} = K(\boldsymbol{p}_s - \boldsymbol{p}) + B(\dot{\boldsymbol{p}}_s - \dot{\boldsymbol{p}}) \tag{6a}$$

where $\boldsymbol{p}_s \in \mathbb{R}^n$ is the position of the proxy, and K and B are the stiffness and the viscosity, respectively, of the virtual coupling. This force $\boldsymbol{f}$ is applied to the controlled object through the actuator. The proxy is also connected to another controller that performs a sliding mode control, which is described as

$$\boldsymbol{f} = F\mathbf{sgn}\left(\boldsymbol{p}_d - \boldsymbol{p}_s + H(\dot{\boldsymbol{p}}_d - \dot{\boldsymbol{p}}_s)\right) \tag{6b}$$

where F and H are positive real numbers, and the function $\mathbf{sgn} : \mathbb{R}^n \to \mathbb{R}^n$ is defined as

$$\mathbf{sgn}(\boldsymbol{x}) \begin{cases} = \boldsymbol{x}/\|\boldsymbol{x}\|, & \text{if } \boldsymbol{x} = \boldsymbol{0} \\ \in \{\boldsymbol{e} \in \mathbb{R}^n \mid \|\boldsymbol{e}\| \le 1\}, & \text{if } \boldsymbol{x} \neq \boldsymbol{0}. \end{cases} \tag{7}$$

Because the proxy is massless, the forces from the virtual coupling and that from the sliding mode controller always balance each other. Thus, both of these forces are denoted as $\boldsymbol{f}$. In other words, the force $\boldsymbol{f}$ is determined so as to satisfy both (6a) and (6b).

The physical meanings of (6b) can be made clear by considering that (6b) is equivalent to

$$\boldsymbol{f} = \lim_{\kappa \to \infty} F\mathbf{sat}\left(\kappa\left(\boldsymbol{p}_d - \boldsymbol{p} + H(\dot{\boldsymbol{p}}_d - \dot{\boldsymbol{p}})\right)/F\right). \tag{8}$$

[1]The terms "proxy" and "virtual coupling" are borrowed from the area of haptic rendering [36], [37].

The equivalency between (6b) and (8) is obvious because of the relation

$$\mathbf{sgn}(\boldsymbol{x}) = \lim_{X \to \infty} \mathbf{sat}(X\boldsymbol{x}) \qquad \forall \boldsymbol{x} \in \mathbb{R}^n. \tag{9}$$

Thus, we can see that the control law (6b) is the force-limited PD control in which the proportional gain is infinite, the time constant is H, and the force limit is F.

Based on the backward Euler approximation, we have the discrete-time representation of (6) as follows:

$$\boldsymbol{f}(k) = K\left(\boldsymbol{p}_s(k) - \boldsymbol{p}(k)\right) + B\frac{\nabla \boldsymbol{p}_s(k) - \nabla \boldsymbol{p}(k)}{T} \tag{10a}$$

$$\boldsymbol{f}(k) = F\mathbf{sgn}\left(\boldsymbol{p}_d(k) - \boldsymbol{p}_s(k) + H\frac{\nabla \boldsymbol{p}_d(k) - \nabla \boldsymbol{p}_s(k)}{T}\right) \tag{10b}$$

where T is the sampling interval, and the argument k in the parentheses is an integer indicating the time index. The operator ∇ is the backward difference operator, which is defined by $\nabla x(k) = x(k) - x(k-1)$. In order to determine $\boldsymbol{f}(k)$ according to a provided $\boldsymbol{p}_d(k)$ and a measured $\boldsymbol{p}(k)$, we have to solve (10). After some derivations [24], we have the computational procedure for solving (10) as follows:

$$\boldsymbol{s}(k) = \left(\boldsymbol{p}_d(k) - \boldsymbol{p}(k)\right) + H\left(\nabla \boldsymbol{p}_d(k) - \nabla \boldsymbol{p}(k)\right)/T \tag{11a}$$

$$\boldsymbol{f}^*(k) = \frac{(B + KT)\boldsymbol{s}(k) + (KH - B)\boldsymbol{e}(k-1)}{H + T} \tag{11b}$$

$$\boldsymbol{f}(k) = F\mathbf{sat}\left(\boldsymbol{f}^*(k)/F\right) \tag{11c}$$

$$\boldsymbol{e}(k) = \frac{B\boldsymbol{e}(k-1) + T\boldsymbol{f}(k)}{B + KT}. \tag{11d}$$

Here, $\boldsymbol{e}(k)$ is the displacement of the proxy with respect to the actual position, i.e., $\boldsymbol{e}(k) = \boldsymbol{p}_s(k) - \boldsymbol{p}(k)$. The algorithm (11) is the control law of PSMC to be implemented in digital controllers.

With setting the stiffness (proportional gain) K to be sufficiently high, the control law (11) of PSMC becomes closer to the force-limited PD control in which the proportional gain is infinite, the time constant is H, and the force limit is F. Because of (11d), $\boldsymbol{e}(k)$ satisfies the following:

$$\boldsymbol{e}(k) = \left(\frac{B}{B + KT}\right)^k \boldsymbol{e}(0) + \sum_{i=0}^{k-1}\left(\frac{B}{B + KT}\right)^{i+1} \frac{T\boldsymbol{f}(k-i)}{B} \tag{12}$$

for all $k \in \{1, 2, \ldots\}$. When we set $\boldsymbol{e}(0) = 0$, the aforementioned expression implies that

$$\lim_{K \to \infty} \boldsymbol{p}_s(k) = \boldsymbol{p}(k) \qquad \forall k \in \{0, 1, 2, \ldots\}. \tag{13}$$

Therefore, because of (10b), the limit of $\boldsymbol{f}(k)$ with $K \to \infty$ becomes as follows:

$$\lim_{K \to \infty} \boldsymbol{f}(k) = F\mathbf{sgn}\left(\boldsymbol{p}_d(k) - \boldsymbol{p}(k) + H\frac{\nabla \boldsymbol{p}_d(k) - \nabla \boldsymbol{p}(k)}{T}\right) \tag{14}$$

for all $k \in \{1, 2, \ldots\}$. Thus, we can see that PSMC can achieve the response characteristics hypothetically preferred for kinesthetic guidance, which are high stiffness and slow response, without using the direct high-gain feedback of the velocity measurements.

Setting $B = KH$ reduces the algorithm (11) into the ordinary PD control scheme with force limit, which is as follows:

$$\boldsymbol{f}^*(k) = K\left(\boldsymbol{p}_d(k) - \boldsymbol{p}(k) + H\frac{\nabla\boldsymbol{p}_d(k) - \nabla\boldsymbol{p}(k)}{T}\right) \quad (15a)$$

$$\boldsymbol{f}(k) = F\mathbf{sat}\left(\boldsymbol{f}^*(k)/F\right). \quad (15b)$$

As mentioned earlier, this control scheme cannot achieve both high stiffness and slow response. The advantage of PSMC (11) over the conventional force-limited PD control (15) can be said to be the separation of large-scale and small-scale responses. A large-scale response can be defined as a response to a large positional error that resulted from actuator force saturation, whereas a small-scale response can be defined as a response to a small positional error that can be recovered without actuator force saturation. The speed of large-scale response depends on H, which should be set around 0.1 s according to the hypothesis in Section II-B. The speed of small-scale response depends on B/K, which should be set small so that $B/K \ll H$ in order to quickly attenuate the influence of small (microscopic) disturbances such as irregular frictional behaviors in the hardware mechanism. That is, K should be chosen as high as permitted by the stability of the controlled system, and B should be chosen small but large enough to suppress oscillation.

The algorithm (11) of PSMC has some possible variations. In a multilinkage mechanism, the force limit should usually be specified in terms of the torque of each actuator. Let us consider a nonredundant rigid manipulator with n degrees of freedom. Let $\boldsymbol{p}$ and $\boldsymbol{p}_d$ denote the actual and desired positions of the end effector in the Cartesian coordinate system, respectively, and $\boldsymbol{f}$ denote the force vector at the end effector that is statically equivalent to the forces from the actuators. Let $\boldsymbol{J} \in \mathbb{R}^{n\times n}$ be the Jacobean matrix that transforms the joint angular velocity to the end-effector velocity in the Cartesian space. Then, the joint actuator torque that is statically equivalent to $\boldsymbol{f}$ is described as $\boldsymbol{\tau} = \boldsymbol{J}^{\mathrm{T}}\boldsymbol{f} \in \mathbb{R}^n$. By using this, we have the modified version of PSMC in which the force limit is specified in terms of the maximum actuator torque, which is written as follows:

$$\boldsymbol{s}(k) = (\boldsymbol{p}_d(k) - \boldsymbol{p}(k)) + H\left(\nabla\boldsymbol{p}_d(k) - \nabla\boldsymbol{p}(k)\right)/T \quad (16a)$$

$$\boldsymbol{f}^*(k) = \frac{(B + KT)\boldsymbol{s}(k) + (KH - B)\boldsymbol{e}(k-1)}{H + T} \quad (16b)$$

$$\boldsymbol{\tau}^*(k) = \boldsymbol{J}(k)^{\mathrm{T}}\boldsymbol{f}^*(k) \quad (16c)$$

$$\boldsymbol{\tau}(k) = \begin{cases} \boldsymbol{\tau}^*(k), & \text{if } \|\boldsymbol{\tau}^*(k)\|_\infty \le F_\tau \\ F_\tau\boldsymbol{\tau}^*(k)/\|\boldsymbol{\tau}^*(k)\|_\infty, & \text{if } \|\boldsymbol{\tau}^*(k)\|_\infty > F_\tau \end{cases} \quad (16d)$$

$$\boldsymbol{f}(k) = \boldsymbol{J}(k)^{-T}\boldsymbol{\tau}(k) \quad (16e)$$

$$\boldsymbol{e}(k) = \frac{B\boldsymbol{e}(k-1) + T\boldsymbol{f}(k)}{B + KT}. \quad (16f)$$

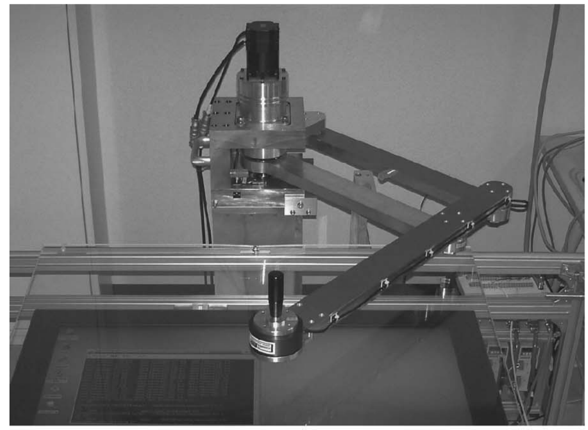

(a)

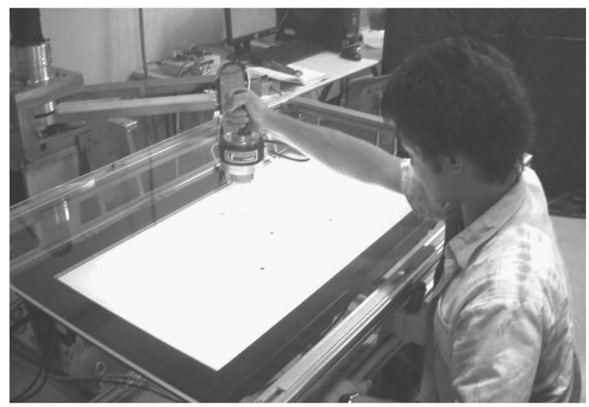

(b)

Fig. 3. Setup for Experiments I and II. (a) Manipulator and LCD monitor. (b) A participant using the manipulator.

Here, $F_\tau > 0$ indicates the limit on the actuator torque, and $\|\boldsymbol{x}\|_\infty$ denotes the L-infinity norm of $\boldsymbol{x} \in \mathbb{R}^n$, which returns $\max_i |x_i|$, where x_i is the ith element of $\boldsymbol{x}$.

III. Experiment I: Positioning

We performed experiments to test the influence of stiffness and the time constant of the position controller in low-force kinesthetic guidance. This section describes the experiments to test its application to a positioning task, and the next section describes that to a trajectory-tracking task. The modified version (16) of PSMC was used as the position controller to produce a wide range of response speed (time constant) combined with high stiffness. We did not compare PSMC with the conventional PD control because the purpose of the experiments was to test the hypothesis in Section II-B and not to demonstrate the advantage of PSMC. The advantage of PSMC over the conventional PD control in combining high stiffness and large time constant has already been demonstrated in a previous paper [24] of the authors.

A. Setup

We used the two-DOF planar parallel manipulator shown in Fig. 3. This manipulator had two actuators on the joints, which were AC servomotors with Harmonic drive gearings.

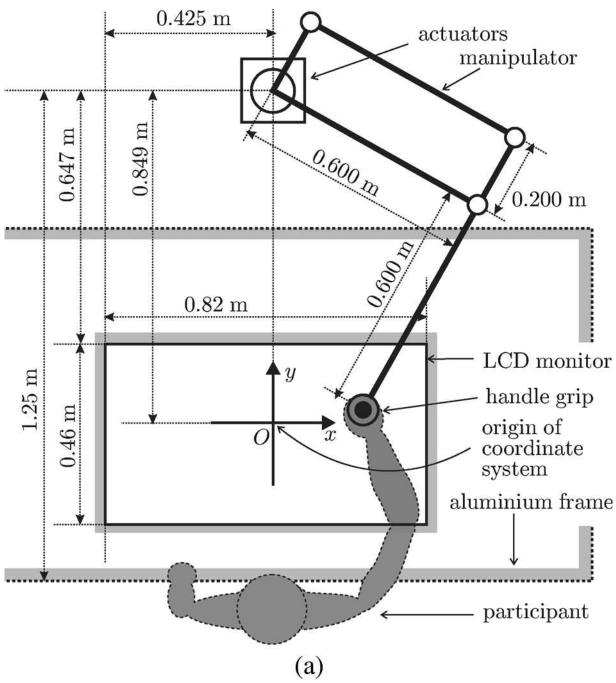

Fig. 4. Dimensions of the setup for Experiments I and II. (a) Top view. (b) Side view.

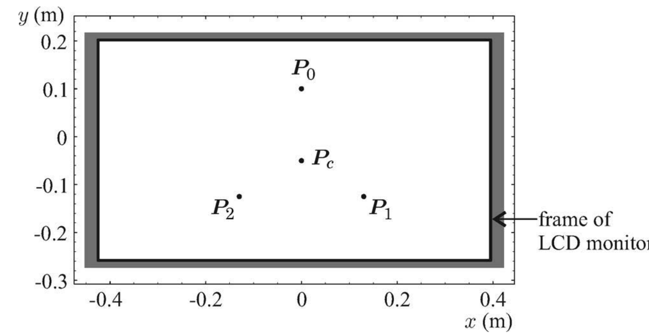

Fig. 5. Graphic representation on the LCD monitor during Experiment I.

TABLE I
PARAMETER SETTINGS USED IN EXPERIMENTS I AND II

name	F_τ (Nm)	H (s)	K (N/m)	B (Ns/m)
C0	0	–	–	–
C1	7	0.5	60000	210
C2	7	0.1	60000	210
C3	7	0.01	60000	210
C4	7	0.1	6000	210
C5	7	0.1	600	210

This manipulator had large friction in its joints; the maximum static friction torque was approximately 10 $\mathrm{N \cdot m}$, and there were some nonuniformities in its distribution. A minimum external force to the end effector that was required to move the end effector depended on the Jacobian matrix $\boldsymbol{J}$, which depended on the end-effector position. At the origin of the coordinate system, at least 16 N of an external force is required to rotate one of the joints and 22 N for both joints. The manipulator also had large link inertia, which also depended on the end-effector position. At the origin, the nominal inertia were approximately 3.0 and 1.3 kg in x and y directions, respectively.

The position of the end effector was measured with two optical encoders attached to the joint actuators. A force sensor was attached to the end effector, and a handle grip was attached to the force sensor. The force sensor was used for measuring the force from a participant, but its measurements were not used in the control algorithm. A 37-in liquid crystal display (LCD) monitor was placed horizontally about 0.2 m below the handle grip. The manipulator and the LCD monitor were arranged as shown in Fig. 4. The whole system was controlled using a personal computer running ART-Linux.

B. Methods and Stimuli

Eight male volunteers participated in Experiment I. All participants were university or graduate students. All of them classified themselves as right handed and had no known injury in their right arms.

During the experiment, the LCD monitor displayed four solid circles with diameters of 0.009 m, as shown in Fig. 5. One of the circles was located at the position $\boldsymbol{P}_c = [0 \text{ m}, -0.05 \text{ m}]^{\mathrm{T}}$. The other three circles $\boldsymbol{P}_0$, $\boldsymbol{P}_1$, and $\boldsymbol{P}_2$ were at the vertices of an equilateral triangle with $0.15 \times \sqrt{3}$ m sides centered at $\boldsymbol{P}_c$. A blue solid circle with a diameter of 0.008 m was drawn immediately below the end effector to indicate the position of the end effector. A "target" was randomly chosen out of $\boldsymbol{P}_0$, $\boldsymbol{P}_1$, and $\boldsymbol{P}_2$, and the participants were asked to move the end effector from $\boldsymbol{P}_c$ to a "target" as quickly as possible. The solid circles at $\boldsymbol{P}_0$, $\boldsymbol{P}_1$, and $\boldsymbol{P}_2$ were drawn in red when chosen as the target and in black if otherwise.

The manipulator was controlled by using the control law described in (16); the end effector's position in the Cartesian coordinate system measured by the optical encoders was used as the input position $\boldsymbol{p}$, and the output torque $\boldsymbol{\tau}$ was commanded to the actuators. Six parameter settings C0 to C5, which are listed in Table I, were used. The sampling interval was $T = 0.001$ s. Notice that the manipulator was not actuated (i.e., the guidance was disabled) in the setting C0. Moreover, notice that the torque limit $F_\tau = 7$ $\mathrm{N \cdot m}$ (in the settings C1 to C5) was lower than the maximum static friction torque in the joints; the manipulator hardly moved without forces from a participant.

A single trial of the experiment was performed in the following procedure.

Step 1) The end effector was fixed at $\boldsymbol{P}_c$.

Step 2) A 3-s countdown was given with beep sounds.

TABLE II
RESULTS OF EXPERIMENT I: TWO-SIDED p-VALUES BASED ON PAIRED t-TESTS ON THE DIFFERENCE IN $\mathcal{T}$

comparison	t-values, df=23	p-values
C3-C2	1.59	1.25×10^{-1}(**)
C2-C1	-16.57	2.78×10^{-14}(**)
C1-C0	-5.26	2.44×10^{-5}(**)
C0-C5	2.97	6.93×10^{-3}(**)
C5-C4	1.56	1.33×10^{-1}(ns)
C4-C2	2.31	2.99×10^{-2}(*)

TABLE III
RESULTS OF EXPERIMENT I: TWO-SIDED p-VALUES BASED ON PAIRED t-TESTS ON THE DIFFERENCE IN $\mathcal{D}$

comparison	t-values, df=23	p-values
C3-C2	5.28	2.36×10^{-5}(**)
C2-C1	-1.75	9.38×10^{-2}(ns)
C1-C0	-4.02	5.37×10^{-4}(**)
C0-C5	7.34	1.82×10^{-7}(**)
C5-C4	3.23	3.70×10^{-3}(**)
C4-C2	1.28	2.15×10^{-1}(ns)

Step 3) At the instant of the "start" beep ($t = 0$), one of the $\boldsymbol{P}_0$ to $\boldsymbol{P}_2$ was chosen as the target and changed its color into red. The control law (11) was activated with one of the settings C0 to C5. The participant moved the end effector to the target.

Step 4) After the end effector's staying within 0.0005 m of the target (i.e., the blue circle's staying within the red circle) for 0.5 s ($t = \mathcal{T}$), the end effector was judged to reach the target.

Step 5) The end effector returned to $\boldsymbol{P}_c$.

The trials were repeated at 3-s intervals. For each trial, the time length $\mathcal{T}$ and the traveled path length $\mathcal{D} = \int_0^{\mathcal{T}} \|\dot{\boldsymbol{p}}(t)\|\, dt$ were recorded.

Every single participant performed 18 trials. All of the 18 possible combinations of the six settings (C0 to C5) and three targets ($\boldsymbol{P}_0$, $\boldsymbol{P}_1$, and $\boldsymbol{P}_2$) were presented to each participant. The order of presentation was randomized for each participant. Prior to the experiment, the participants performed at least 18 unrecorded trials as practice.

According to the hypothesis in Section II-B, $H = 0.1$ s and a higher K are expected to be suitable for kinesthetic guidance. Thus, the setting C2 is expected to be the best among the six settings in Table I. The proportional gain of $K = 60\,000$ N/m was close to the highest value with which the entire system was stable.

C. Results

The total number of trials under each setting of C0 to C5 was 24 (three targets × eight participants). The obtained data of the time $\mathcal{T}$ and the path length $\mathcal{D}$ were analyzed by using paired t-test based on the pairs of data from different settings, the same target, and the same participant. This is because the data can be influenced not only by the parameter settings but also by the choice of targets and the physical capability of participants. The p-values for the comparisons are shown in Tables II and III. Here, the single asterisk (*) and double asterisk (**) indicate significant differences at $p < 0.05$ and $p < 0.01$, respectively, and ns indicates no significant difference ($p \geq 0.05$).

Fig. 6 shows the averages and the standard deviations of the time $\mathcal{T}$ and the path length $\mathcal{D}$ under the settings C0 to C5. Note that these averages and standard deviations are not used in the statistical analysis because the paired t-tests were performed by basing on the paired differences. The data are arranged in an order that is convenient for comparison, and the result with the setting C2 is presented at two places. The asterisks indicate the results of the statistical analysis, which are also presented in Tables II and III.

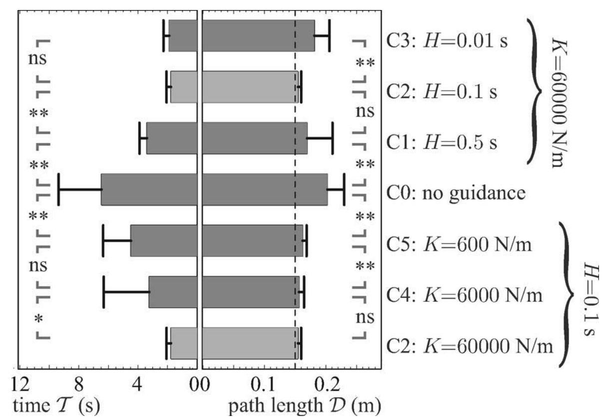

Fig. 6. Results of Experiment I: Averages and standard deviations of $\mathcal{T}$ and $\mathcal{D}$. These values are not used in the statistical analysis but are shown for reference only. The vertical dotted line in the right pane indicates the direct distance of the targets, which is 0.15 m. The result with C2 ($K = 60\,000$ N/m, and $H = 0.1$ s) is presented at two places for the convenience of comparison.

Tables II and III and Fig. 6 show that the performance under the setting C0 is significantly worse than those under the other settings. This means that even a small guiding force below the maximum static friction level is capable of improving the efficiency of positioning tasks.

The result of the setting C2 ($H = 0.1$ s) is better than those of the settings C1 and C3, which have the same K value but different H values. This result supports our hypothesis in Section II-B. The difference between C2 and C3 is not significant in time length $\mathcal{T}$, but it is significant in the path length $\mathcal{D}$. This indicates that a small H value ($H = 0.01$ s in C3) can increase the speed of the reaching movement but can cause overshoots. The comparisons C2–C4 and C4–C5 suggest that a large K value is desirable for guiding positioning tasks. This is probably because, as the K value increases, the force attracting the end effector to the target becomes larger up to the saturation level determined by F_τ.

Fig. 7 shows the typical example data of motions from $\boldsymbol{P}_c$ to $\boldsymbol{P}_0$ performed by one of the participants. It is apparent that the position approaches to the target $\boldsymbol{P}_0$ faster under the setting C3 than under the setting C2, but the setting C3 results in an overshoot. The setting C2 creates more smooth and efficient motions than the settings C0, C1, and C3. Fig. 8 shows the data of the motion and the participant's force measured in the same trials as Fig. 7. It shows that, under the setting C0 (no guidance), the participant's force is fluctuating at the target $\boldsymbol{P}_0$ probably due to his effort of final fine positioning. The setting C1 causes a larger force because it produces resisting actuator forces to decelerate the motion. Under the setting C2, the participant

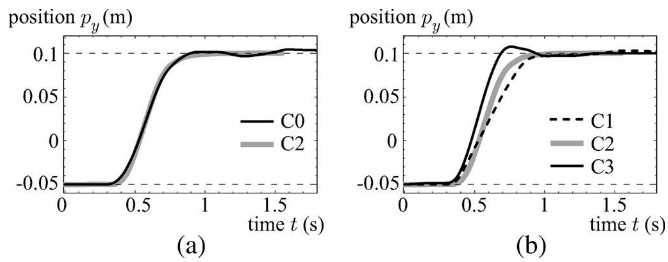

Fig. 7. Typical examples of the measured position data (from $\boldsymbol{P}_c$ to $\boldsymbol{P}_0$) in Experiment I. The data are distributed into two figures for the convenience of comparison. (a) C0 and C2. (b) C1, C2, and C3.

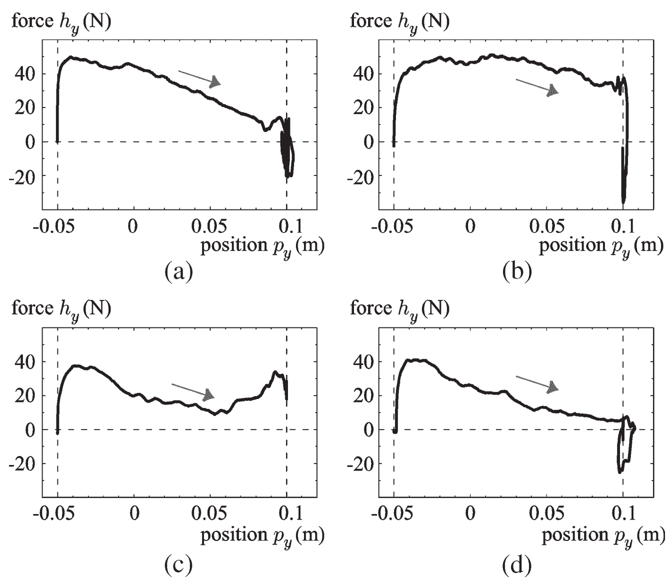

Fig. 8. Typical examples of the measured data of position and force in Experiment I. The force data are the forces applied from the participant to the force sensor. (a) C0: No guidance. (b) C1: $H = 0.5$ s. (c) C2: $H = 0.1$ s. (d) C3: $H = 0.01$ s.

makes almost no effort of final fine positioning. Although such qualitative observations can be made, the establishment of reliable quantitative measures based on force data is left for future study.

IV. Experiment II: Trajectory Tracking

We performed another experiment to test the influence of stiffness and the time constant of position control onto the performance of trajectory tracking. We also used the setup introduced in Section III-A and shown in Figs. 3 and 4. The control law (16) was used also in this experiment with the parameter settings C0 to C5 in Table I.

A. Methods and Stimuli

Eight male volunteers participated in this experiment. All participants were university or graduate students. All of them classified themselves as right handed and had no known injury in their right arms.

In this experiment, the desired trajectory to be tracked was chosen as a Lissajou's trajectory described as follows:

$$\boldsymbol{p}_d(t) = [A_x \sin(\Omega t), A_y \sin(2\Omega t) + B_y]^{\mathrm{T}} \tag{17}$$

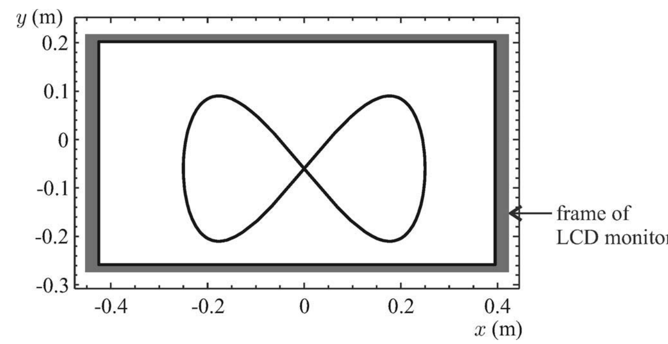

Fig. 9. Graphic representation on the LCD monitor during Experiment II.

where $A_x = 0.25$ m, $A_y = 0.15$ m, $B_y = -0.06$ m, $\Omega = 0.5\ \pi$ rad/s. This trajectory was drawn as a red solid curve on the LCD monitor, as shown in Fig. 9. The desired position $\boldsymbol{p}_d$ at each time instant was indicated by a solid red circle with a diameter of 0.012 m. In addition, a solid blue circle with a diameter of 0.008 m was drawn immediately below the end effector to indicate the measured end-effector position $\boldsymbol{p}$. A single trial of the experiment includes two laps around the trajectory (i.e., $t \in [0, 8\ \mathrm{s}]$).

A single trial of this experiment was performed in the following procedure.

Step 1) The end-effector position was fixed at the position $[0, B_y]^{\mathrm{T}}$.

Step 2) A 3-s countdown was given with beep sounds.

Step 3) At the instant of the "start" beep ($t = 0$), the red circle started to move along the trajectory (17). The control law (11) was activated with one of the settings C0 to C5. The participant started to move the end effector to follow the red circle as accurately as possible.

Step 4) After two cycles ($t = 8$ s), the end effector stopped at the position $[0, B_y]^{\mathrm{T}}$.

The trials were repeated at 3-s intervals. Every single participant performed six trials. All of the six settings (C0 to C5) were presented to each participant. The order of presentation was randomized for each participant. Prior to the experiment, the participants performed at least six unrecorded trials as practice.

B. Results

We chose the following criterion for evaluating the tracking accuracy in a single trial:

$$\mathcal{L} = \frac{1}{t_1 - t_0} \int_{t_0}^{t_1} \log_{10} \left(\|\boldsymbol{p}(t) - \boldsymbol{p}_d(t)\| \right) \, dt \tag{18}$$

where $t_0 = 0.2$ s, $t_1 = 7.8$ s, and $\|\boldsymbol{p}(t) - \boldsymbol{p}_d(t)\|$ is measured in meters (m).

The total number of trials under each setting of C0 to C5 was eight (one trial $\times$ eight participants). The obtained data of the $\mathcal{L}$ value were analyzed by using paired t-test based on the pairs of data from different settings and the same participant. The p-values for the comparisons are shown in Table IV.

TABLE IV
RESULTS OF EXPERIMENT II: TWO-SIDED p-VALUES BASED ON PAIRED t-TESTS ON THE DIFFERENCE IN $\mathcal{L}$

comparison	t-values, df=7	p-values
C3-C2	3.56	9.25×10^{-3}(**)
C2-C1	-2.38	4.86×10^{-2}(*)
C1-C0	-6.12	4.82×10^{-4}(**)
C0-C5	7.73	1.14×10^{-4}(**)
C5-C4	4.47	2.91×10^{-3}(**)
C4-C2	2.99	2.03×10^{-2}(*)

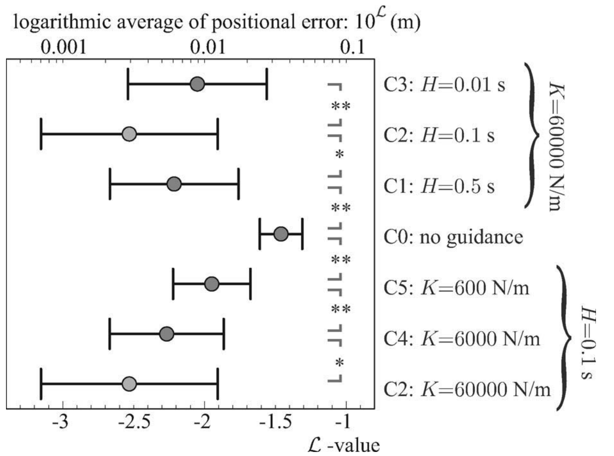

Fig. 10. Results of Experiment II: Averages and standard deviations of $\mathcal{L}$. These values are not used in the statistical analysis but are shown for reference only. The result with C2 ($K = 60\ 000$ N/m, and $H = 0.1$ s) is presented at two places for the convenience of comparison.

Fig. 10 shows the averages and the standard deviations of the $\mathcal{L}$ values under the settings C0 to C5. Again, note that these averages and standard deviations are not used in the statistical analysis. The data are arranged in the same order as in Fig. 6. The asterisks indicate the results of the statistical analysis.

Table IV and Fig. 10 show that the setting C2 created better results than the other settings. The results show that, in order to reduce the tracking error, the proportional gain K should be chosen high and the time constant H should be around 0.1 s. It is consistent with our hypothesis in Section II-B.

Fig. 11 shows the typical example data of motions produced by one of the participants. It is apparent that the setting C2 produces a better result than C0 and C3, and the setting C3 results in repeated overshoots. The difference between C1 and C2 is not apparent in Fig. 11, but it is already shown in Table IV and Fig. 10.

As a supplementary experiment, we tried the parameter setting $F_\tau = 7$ N $\cdot$ m, $K = 60\ 000$ N/m, $B = 6000$ N $\cdot$ s/m, and $H = 0.1$ s. This parameter setting is the same in K and H as the setting C2, but because of $H = B/K$, it makes the control law to be equivalent to the ordinary torque-limited PD control law, as explained in Section II-C. With this parameter setting, the actuator often created undesirable noisy sound, particularly when the end-effector position was very close to the desired position and the velocity was very low. It is probably because the large B value amplified the influence of the measurement noise in the velocity signal. This indicates that PSMC is a necessary choice to realize an appropriately large time constant and a high stiffness.

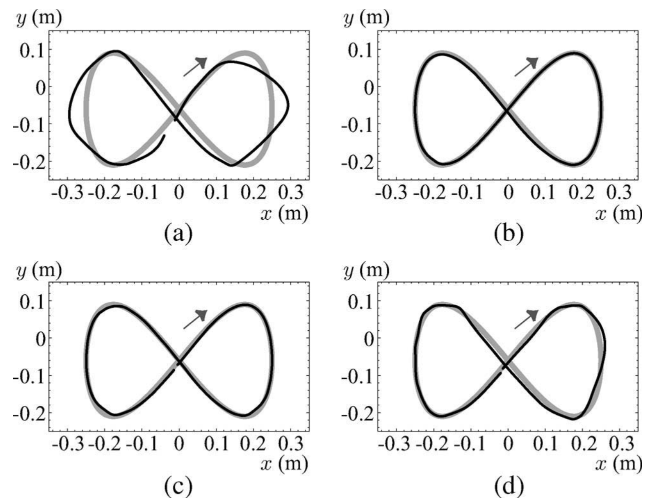

Fig. 11. Typical data of motions produced by a participant in Experiment II. (Thick gray curves represent the desired trajectories.) (a) C0: No guidance. (b) C1: $H = 0.5$ s. (c) C2: $H = 0.1$ s. (d) C3: $H = 0.01$ s.

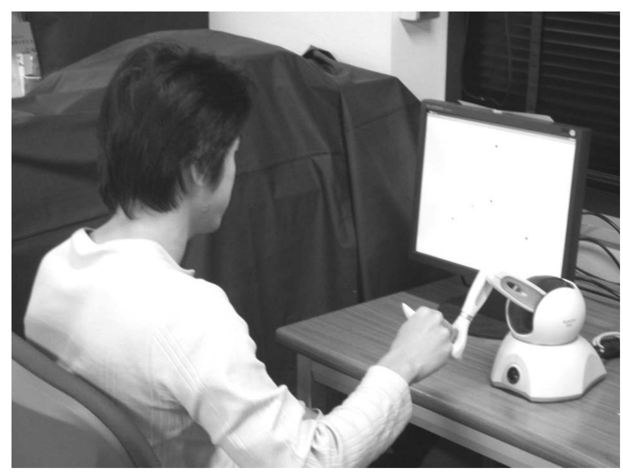

Fig. 12. Setup for Experiments III and IV.

V. EXPERIMENTS III AND IV: POSITIONING AND TRAJECTORY TRACKING USING A LIGHTWEIGHT DEVICE

Because the experimental results obtained so far are based on a single specific device, there still remains a possibility that the appropriate time constant, which is 0.1 s, may not be a characteristic of humans but of the device used in the experiments. In order to reduce this possibility and strengthen the support for the hypothesis in Section II-B, we performed another two sets of experiments with a robotic device that was distinctly different from the device used in Experiments I and II.

A. Setup

We used the experimental setup shown in Figs. 12 and 13. It is composed of a SensAble PHANTOM Omni haptic device and a 17-in LCD monitor. The haptic device was capable of three degree-of-freedom actuation and six degree-of-freedom measurements. Because it was difficult to match the end-effector position to a specified position in the 3-D space, all

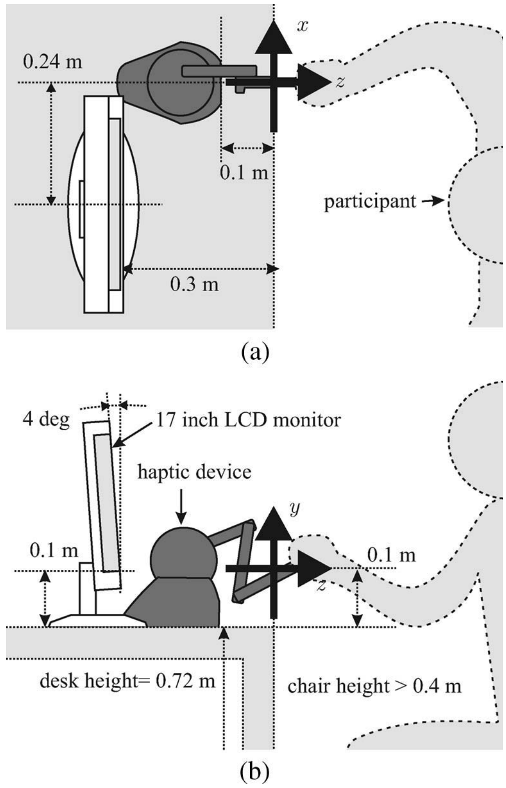

Fig. 13. Dimensions of the setup for Experiments III and IV. (a) Top view. (b) Side view.

TABLE V
PARAMETER SETTINGS USED IN EXPERIMENTS III AND IV

name	F (N)	H (s)	K (N/m)	B (Ns/m)
C0	0	–	–	–
C1	1.0	0.5	800 (400 for Exp.IV)	0
C2	1.0	0.1	800 (400 for Exp.IV)	0
C3	1.0	0.01	800 (400 for Exp.IV)	0
C4	1.0	0.1	80	0
C5	1.0	0.1	8	0

tasks were performed and evaluated in the $x{-}y$ plane, which was parallel to the screen of the LCD monitor.

The end effector was controlled to stay on the $x{-}y$ plane by using the ordinary proportional control with respect to the z coordinate with a proportional gain of 700 N/m. The $x{-}y$ coordinate of the end effector was controlled by using PSMC in the Cartesian coordinate, which is (11). The parameter sets were defined as in Table V. Due to technical reasons concerning the stability of the device, the proportional gain K in Experiment IV was set lower. Note that the force in z direction is not limited, whereas the magnitude of the force in $x{-}y$ plane is limited by F in Table V. The sampling interval was set to be $T = 1/1600 = 0.000625$ s.

During the experiments, the measured position of the end effector and the desired positions (in the $x{-}y$ plane) were indicated by solid circles on the LCD monitor. The origin of the coordinate system was matched to the center of the LCD monitor. The motion of the end effector was mapped at the same scale on the LCD monitor.

The participants were asked not to put their elbows on the desk during trials. They were also asked to firmly grasp the stylus in a pen-hold posture, because a loosely grasped stylus can be easily moved by the forces from the haptic device without inducing any motion in the participant's hand.

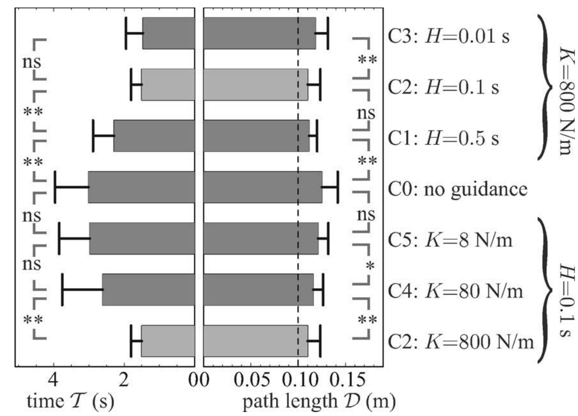

Fig. 14. Results of Experiment III: Averages and standard deviations of $\mathcal{T}$ and $\mathcal{D}$. These values are not used in the statistical analysis but are shown for reference only. The vertical dotted line in the right pane indicates the direct distance of the targets, which is 0.10 m. The result with C2 ($K = 800$ N/m, and $H = 0.1$ s) is presented at two places for the convenience of comparison.

TABLE VI
RESULTS OF EXPERIMENT III: TWO-SIDED p-VALUES BASED ON PAIRED t-TESTS ON THE DIFFERENCE IN $\mathcal{T}$

comparison	t-values, df=41	p-values
C3-C2	-0.43	6.71×10^{-1}(ns)
C2-C1	-7.28	6.55×10^{-9}(**)
C1-C0	-4.15	1.64×10^{-4}(**)
C0-C5	0.22	8.31×10^{-1}(ns)
C5-C4	1.83	7.38×10^{-2}(ns)
C4-C2	6.14	2.71×10^{-7}(**)

B. Experiment III: Positioning

Experiment III was performed in mostly the same manner as Experiment I. The differences from Experiment I are listed hereafter.

1) The targets were placed at the vertices of an equilateral triangle with $0.10 \times \sqrt{3}$ m sides centered at $\boldsymbol{P}_c = [0, 0 \text{ m}]$.
2) The targets were 0.005 m in diameters, and the blue circle, which is the indicator of the end-effector position $\boldsymbol{p}$, was 0.004 m in diameter.
3) In the end effector's staying within 0.001 m of the target (i.e., the blue circle's staying within the red circle) for 0.5 s ($t = \mathcal{T}$), the end effector was judged to reach the target.

Fourteen male volunteers participated in this experiment.

The results are shown in Tables VI and VII and Fig. 14. The relations among the parameter settings C0, C1, C2, and C3 are almost the same as those in Experiment I. There is no significant difference between C0 and C5, but it will probably be because the stiffness of 8 N/m is too low. These results support the hypothesis that the stiffness should be high and the time constant should be 0.1 s rather than 0.01 and 0.5 s.

TABLE VII
RESULTS OF EXPERIMENT III: TWO-SIDED p-VALUES BASED ON PAIRED t-TESTS ON THE DIFFERENCE IN $\mathcal{D}$

comparison	t-values, df=41	p-values
C3-C2	2.80	7.68×10^{-3}(**)
C2-C1	-0.56	5.79×10^{-1}(ns)
C1-C0	-4.49	5.70×10^{-5}(**)
C0-C5	1.64	1.08×10^{-1}(ns)
C5-C4	2.40	2.09×10^{-2}(*)
C4-C2	2.81	7.65×10^{-3}(**)

C. Experiment IV: Trajectory Tracking

The procedure of Experiment IV was mostly the same as Experiment II. The differences are listed hereafter.

1) The desired trajectory was chosen as (17), where the parameters were set as $A_x = 0.085$ m, $A_y = 0.051$ m, $B_y = 0$ m, $\Omega = 1.25\ \pi\mathrm{rad/s}$. Thus, the time length for one trial (two cycles) was 3.2 s.
2) The red circle (the indicator of the desired position $\boldsymbol{p}_d$) was 0.005 m in diameter, and the blue circle (the indicator of the tool position $\boldsymbol{p}$) was 0.004 m in diameter.

Eighteen male volunteers and one female volunteer participated in this experiment.

The obtained data are evaluated by using the $\mathcal{L}$-value criterion defined in (18), where $t_0 = 0.08$ s and $t_1 = 3.12$ s. The results are shown in Table VIII and Fig. 15. As is apparent, the difference between C3 and C2 is not significant. This is probably because C3 and C2 (having the same K but different H) do not make any difference after a sufficient time elapses because the force $\boldsymbol{f}$ comes below the saturation level F. This is also the case with the parameter setting C1, but a time constant of 0.5 s may not be short enough compared to the cycle of the motion (1.6 s) or the time length of the trial (3.2 s). As a characteristic of PSMC (see Fig. 2), when $\boldsymbol{f}$ is being smaller than F for a sufficient time, the proxy position $\boldsymbol{p}_s$ almost coincides with the desired position $\boldsymbol{p}_d$, and thus, the behavior of the tool position $\boldsymbol{p}$ is governed only by the virtual coupling, which depends on K and has nothing to do with H. Once the tool was "locked" to the target (i.e., the proxy reached the target), in this experimental condition, it was not so difficult for participants to keep moving along the target $\boldsymbol{p}_d$ because of almost homogenous friction and inertia of the device. The dotted line in Fig. 15 shows the displacement $1.0/400 = 0.0025$ m, which is the maximum allowed length F/K of the virtual coupling in the parameter settings C1, C2, and C3. In average, the positional error $\|\boldsymbol{p}_d - \boldsymbol{p}\|$ was below F/K for 35% and 34% of the time periods of the trials with the settings C3 and C2, respectively. This implies that the participants succeeded to maintain accurate tracking for considerable lengths of time with the actuator forces unsaturated.

Nevertheless, the results show that the reduction of H has little effect below 0.1 s, and thus, we can conclude that the time constant should be set around 0.1 s, when the actuator force saturation is probable.

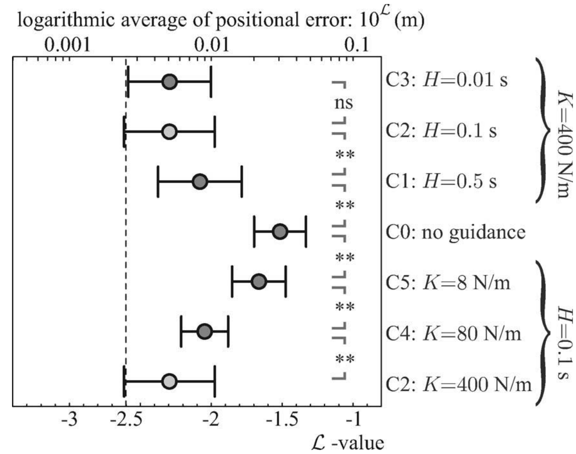

Fig. 15. Results of Experiment IV: Averages and standard deviations of $\mathcal{L}$. These values are not used in the statistical analysis but are shown for reference only. The dotted line represents the displacement $1.0/400 = 0.0025$ m, which is the maximum allowed length F/K of the virtual coupling in the parameter settings C1, C2, and C3. The result with C2 ($K = 400$ N/m, and $H = 0.1$ s) is presented at two places for the convenience of comparison.

TABLE VIII
RESULTS OF EXPERIMENT IV: TWO-SIDED p-VALUES BASED ON PAIRED t-TESTS ON THE DIFFERENCE IN $\mathcal{L}$

comparison	t-values, df=18	p-values
C3-C2	0.03	9.79×10^{-1}(ns)
C2-C1	-3.03	7.21×10^{-3}(**)
C1-C0	-8.91	5.09×10^{-8}(**)
C0-C5	3.73	1.53×10^{-3}(**)
C5-C4	8.98	4.53×10^{-8}(**)
C4-C2	4.41	3.38×10^{-4}(**)

VI. CONCLUSION

This paper has considered the application of a low-force robotic manipulator to guide a human user's positioning or trajectory-tracking tasks toward a predetermined desired position or trajectory. We hypothesized that the position controller for low-force kinesthetic guidance should be as follows:

1) as stiff as possible;
2) as slow as approximately 0.1 s in terms of time constant.

Experiments were performed to validate the aforementioned hypothesis by using the authors' recent technique, which is the PSMC [24], because ordinary PD control has technical limitations to realize the aforementioned preferred characteristics. The experimental results from two distinctly different robotic devices supported the hypothesis, showing that a time constant of 0.1 s was better than 0.01 and 0.5 s in most cases. However, when the task was not so difficult as to result in the constant or frequent saturation of the actuator forces, the difference between 0.1 and 0.01 s was not apparent. Nevertheless, we can conclude that a time constant of around 0.1 s is desirable at least when the actuator force saturation is probable.

Although this paper limited its scope to empirical validation of the hypothesis, attempts should be made to clarify physical and physiological mechanisms that can explain the hypothesis and the experimental results. The relation between the neuromuscular dynamics [28], [38] and the physical dynamics of human movements may still need some clarifications, which will require nonlinear system and optimal control theories.

The preferred choice of the time constant (H-value) should be investigated from both empirical and theoretical points of view. It may be related to the frequency or impedance characteristics of human muscles and motor control strategies [39]–[41]. Moreover, the sensitivity of the human performance against the choice of H-value will be an important topic of study. A more precise identification of the preferred H-value may contribute to a better human–machine coordination.

We expect that the results obtained in this paper provide some insights regarding rehabilitation robotics, particularly for active-assistive exercise. The recent robotic devices for active-assistive rehabilitation employ impedance control [19], [20] or position control along a preprogrammed smooth trajectory [21], [22]. To the best of the authors' knowledge, the literature includes no studies regarding the influence of the choice of the damping (the velocity feedback gain) in this application. Slow overdamped responses produced by PSMC may be effective for this application, although the effectiveness will need to be evaluated through more reliable performance measures other than reaching time and average positional errors. The application of PSMC for guiding different portions of the human body, such as lower limbs [42], will also be an important topic.

ACKNOWLEDGMENT

The authors would like to thank Prof. N. Takesue of Nagoya Institute of Technology, who designed and constructed the experimental setup consisting of the parallel link manipulator and the LCD monitor, the students of Nagoya Institute of Technology who shared their time by participating in the experiments, and the engineers of Toyota Motor Corporation who motivated this research.

REFERENCES

[1] R. Kikuuwe, T. Yamamoto, and H. Fujimoto, "Low-force kinesthetic guidance for accurate positioning and tracking," in *Proc. 14th Symp. Haptic Interfaces Virtual Environ., Teleoperator Syst.*, 2006, pp. 491–498.

[2] H. Kazerooni, "Human–robot interaction via the transfer of power and information signals," *IEEE Trans. Syst., Man, Cybern.*, vol. 20, no. 2, pp. 450–463, Mar./Apr. 1990.

[3] T. Tsumugiwa, R. Yokogawa, and K. Hara, "Variable impedance control based on estimation of human arm stiffness for human–robot cooperative calligraphic task," in *Proc. IEEE Int. Conf. Robot. Autom.*, 2002, pp. 644–650.

[4] Y. Yamada, H. Konosu, T. Morizono, and Y. Umetani, "Proposal of skill-assist: A system of assisting human workers by reflecting their skills in positioning tasks," in *Proc. IEEE Int. Conf. Syst., Man, Cybern.*, 1999, vol. 4, pp. 11–16.

[5] R. Ikeura, T. Moriguchi, and K. Mizutani, "Optimal variable impedance control for a robot and its application to lifting an object with a human," in *Proc. 11th IEEE Int. Workshop Robot Human Interactive Commun.*, 2002, pp. 500–505.

[6] Y. Hirata, T. Takagi, K. Kosuge, H. Asama, H. Kaetsu, and K. Kawabata, "Motion control of multiple DR helpers transporting a single object in cooperation with a human based on map information," in *Proc. IEEE Int. Conf. Robot. Autom.*, 2002, pp. 995–1000.

[7] C. Richard and M. R. Cutkosky, "The effects of real and computer generated friction on human performance in a targeting task," in *Proc. 8th Symp. Haptic Interfaces Virtual Environ., Teleoperator Syst.*, 2000, pp. 1101–1108.

[8] D. W. Repperger and D. McCollor, "Active sticks: A new dimension in controller design," in *Proc. 20th Annu. Conf. Manual Control*, 1984, vol. 1, pp. 719–734.

[9] J. Pracher, A. Cozzone, D. W. Repperger, and D. Norman, "Information theory analysis of human tracking performance using a smart stick controller," in *Proc. IEEE Nat. Aerosp. Electron. Conf.*, 1989, vol. 4, pp. 1843–1850.

[10] R. B. Gillespie, J. E. Colgate, and M. A. Peshkin, "A general framework for cobot control," *IEEE Trans. Robot. Autom.*, vol. 17, no. 4, pp. 391–401, Aug. 2001.

[11] A. Bettini, P. Marayong, S. Lang, A. M. Okamura, and G. D. Hager, "Vision-assisted control for manipulation using virtual fixtures," *IEEE Trans. Robot.*, vol. 20, no. 6, pp. 953–966, Dec. 2004.

[12] J. J. Abbott and A. M. Okamura, "Stable forbidden-region virtual fixtures for bilateral telemanipulation," *Trans. ASME, J. Dyn. Syst. Meas. Control*, vol. 128, no. 1, pp. 53–64, Mar. 2006.

[13] R. Kikuuwe, N. Takesue, and H. Fujimoto, "Passive virtual fixtures based on simulated position-dependent anisotropic plasticity," in *Proc. IEEE Int. Conf. Robot. Autom.*, 2007, pp. 3263–3268.

[14] D. Feygin, M. Keehner, and F. Tendick, "Haptic guidance: Experimental evaluation of a haptic training method for a perceptual motor skill," in *Proc. 10th Symp. Haptic Interfaces Virtual Environ., Teleoperator Syst.*, 2002, pp. 40–47.

[15] R. Kikuuwe and T. Yoshikawa, "Haptic display device with fingertip presser for motion/force teaching to human," in *Proc. IEEE Int. Conf. Robot. Autom.*, 2001, pp. 868–873.

[16] M. K. O'Malley, A. Gupta, M. Gen, and Y. Li, "Shared control in haptic systems for performance enhancement and training," *Trans. ASME, J. Dyn. Syst. Meas. Control*, vol. 128, no. 1, pp. 75–85, Mar. 2006.

[17] Y. Yokokohji, R. L. Hollis, T. Kanade, K. Henmi, and T. Yoshikawa, "Toward machine mediated training of motor skills: Skill transfer from human to human via virtual environment," in *Proc. IEEE Int. Workshop Robot Human Interactive Commun.*, 1996, pp. 32–37.

[18] B. A. C. Forsyth and K. E. MacLean, "Predictive haptic guidance: Intelligent user assistance for the control of dynamic tasks," *IEEE Trans. Vis. Comput. Graphics*, vol. 12, no. 1, pp. 103–113, Jan./Feb. 2006.

[19] M. Casadio, P. G. Morasso, V. Sanguineti, and P. Giannoni, "Impedance-controlled, minimally-assistive robotic training of severely impaired hemiparetic patients," in *Proc. 1st IEEE/RAS-EMBS Int. Conf. Biomed. Robot. Biomechatronics*, 2006, pp. 507–512.

[20] H. I. Krebs, N. Hogan, M. L. Aisen, and B. T. Volpe, "Robot-aided neurorehabilitation," *IEEE Trans. Rehabil. Eng.*, vol. 6, no. 1, pp. 75–87, Mar. 1998.

[21] D. J. Reinkensmeyer, J. P. A. Dewald, and W. Z. Rymer, "Guidance-based quantification of arm impairment following brain injury: A pilot study," *IEEE Trans. Rehabil. Eng.*, vol. 7, no. 1, pp. 1–11, Mar. 1999.

[22] Y. Tanaka, T. Tsuji, and M. Kaneko, "A bio-mimetic rehabilitation aid for motor control training using time base generator," in *Proc. 26th Annu. Conf. IEEE Ind. Electron. Soc.*, 2000, pp. 114–119.

[23] J. J. Abbott and A. M. Okamura, "Effects of position quantization and sampling rate on virtual-wall passivity," *IEEE Trans. Robot.*, vol. 21, no. 5, pp. 952–964, Oct. 2005.

[24] R. Kikuuwe and H. Fujimoto, "Proxy-based sliding mode control for accurate and safe position control," in *Proc. IEEE Int. Conf. Robot. Autom.*, 2006, pp. 26–31.

[25] P. Morasso, "Spatial control of arm movements," *Exp. Brain Res.*, vol. 42, no. 2, pp. 223–227, Apr. 1981.

[26] W. Abend, E. Bizzi, and P. Morasso, "Human arm trajectory formation," *Brain*, vol. 105, pp. 331–348, Jun. 1982.

[27] R. Happee, "Goal-directed arm movements: II. A kinematic model and its relation to EMG records," *J. Electromyogr. Kinesiol.*, vol. 3, no. 1, pp. 13–23, 1993.

[28] D. L. Kleinman, S. Baron, and W. H. Levison, "A control theoretic approach to manned-vehicle systems analysis," *IEEE Trans. Autom. Control*, vol. AC-16, no. 6, pp. 824–832, Dec. 1971.

[29] D. P. Miller and E. W. Vinje, "Fixed-base flight simulator studies of VTOL aircraft handling qualities in hovering and low-speed flight," Air Force Flight Dynamic Lab., Dayton, OH, Tech. Rep. AFFDL-TR-67-152, 1968.

[30] K. A. Mann, F. W. Wernere, and A. K. Palmer, "Frequency spectrum analysis of wrist motion for activities of daily living," *J. Orthopaedic Res.*, vol. 7, no. 2, pp. 304–306, 1989.

[31] J. M. Hollerbach, "An oscillation theory of handwriting," *Biol. Cybern.*, vol. 39, no. 2, pp. 139–156, Jan. 1981.

[32] C. N. Riviere, R. S. Rader, and P. K. Khosla, "Characteristics of hand motion of eye surgeons," in *Proc. 19th Annu. Conf. IEEE Eng. Med. Biol. Soc.*, 1997, vol. 4, pp. 1690–1693.

[33] M. Goldfarb and T. Sirithanapipat, "The effect of actuator saturation on the performance of PD-controlled servo systems," *Mechatronics*, vol. 9, no. 5, pp. 497–511, Aug. 1999.

[34] P. T. Larsson and A. G. Ulsoy, "Fast control of linear systems subject to input constraints," *Trans. ASME, J. Dyn. Syst. Meas. Control*, vol. 122, no. 1, pp. 18–26, Mar. 2000.

[35] F. Janabi-Sharifi, V. Hayward, and C.-S. J. Chen, “Discrete-time adaptive windowing for velocity estimation,” *IEEE Trans. Control Syst. Technol.*, vol. 8, no. 6, pp. 1003–1009, Nov. 2000.
[36] J. E. Colgate, M. C. Stanley, and J. M. Brown, “Issues in the haptic display of tool use,” in *Proc. IEEE/RSJ Int. Conf. Intell. Robots Syst.*, 1995, vol. 3, pp. 140–145.
[37] D. C. Ruspini, K. Kolarov, and O. Khatib, “The haptic display of complex graphical environments,” in *Proc. 24th Annu. Conf. Comput. Graph. Interactive Techn.*, 1997, pp. 345–352.
[38] D. McRuer, “Human dynamics in man–machine systems,” *Automatica*, vol. 16, no. 3, pp. 237–253, 1980.
[39] G. I. Zahalak and S. J. Heyman, “A quantitative evaluation of the frequency-response characteristics of active human skeletal muscle *in vivo*,” *Trans. ASME, J. Biomech. Eng.*, vol. 101, pp. 28–37, 1979.
[40] N. Hogan, “Adaptive control of mechanical impedance by coactivation of antagonist muscles,” *IEEE Trans. Autom. Control*, vol. AC-29, no. 8, pp. 681–690, Aug. 1984.
[41] T. Tsuji and Y. Tanaka, “Tracking control properties of human-robotic systems based on impedance control,” *IEEE Trans. Syst., Man, Cybern. A, Syst., Humans*, vol. 35, no. 4, pp. 523–535, Jul. 2005.
[42] H. Toda, T. Kobayakawa, and Y. Sankai, “A multi-link system control strategy based on biological reaching movement,” *Adv. Robot.*, vol. 20, no. 6, pp. 661–679, Jun. 2006.

Ryo Kikuuwe (S’02–M’03) received the B.S., M.S., and Ph.D. (Eng.) degrees in mechanical engineering from Kyoto University, Kyoto, Japan, in 1998, 2000, and 2003 respectively.

From 2003 to 2007, he was an Endowed-Chair Research Associate with the Nagoya Institute of Technology, Nagoya, Japan. He is currently an Associate Professor with Kyushu University, Fukuoka, Japan. His research interests include human–robot coordination, real-time simulation for haptic rendering and physics-based animation, and tactile sensing.

Dr. Kikuuwe is a member of the Robotics Society of Japan, the Japan Society of Mechanical Engineers, the Society of Instrument and Control Engineers (Japan), and the Virtual Reality Society of Japan.

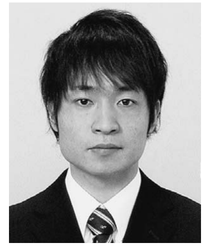

Takahiro Yamamoto received the B.E. degree in mechanical engineering from the Nagoya Institute of Technology, Nagoya, Japan, in 2006, where he is working toward the M.S. degree in engineering.

Mr. Yamamoto is a Student Member of the Robotics Society of Japan.

Hideo Fujimoto received the B.M.E. degree from Nagoya University, Nagoya, Japan, in 1970, where he received the Ph.D. degree in engineering.

He is currently a Professor with the Graduate School of Engineering, Nagoya Institute of Technology, Nagoya, where he is the Director of the Quality Innovation Techno-Center. His main research interests are production systems, intelligent robots, virtual reality, and sensitive engineering.

Prof. Fujimoto is a Fellow of the Japan Society of Mechanical Engineers, a Standing Director and the Council Chair of the Society of Instrument and Control Engineers, and the President of the Scheduling Society of Japan. He received the Best Paper Award for a paper presented at the Japan–USA Flexible Automation Symposium 2000; the Best Paper Award at the 6th Robotics Symposium; the Contribution Award from the System Integration Section, Society of Instrument and Control Engineers; and the Great Contribution Award from the Production System Section, Japan Society of Mechanical Engineers in 2002.